CHARACTERIZATION OF THE COHERENT NOISE, ELECTROMAGNETIC COMPATIBILITY AND ELECTROMAGNETIC INTERFERENCE OF THE ATLAS EM CALORIMETER FRONT END BOARD*

R. L. Chase, M. Citterio, F. Lanni,
D. Makowiecki, V. Radeka, S. Rescia, and H. Takai

Brookhaven National Laboratory, Upton, NY 11973

J. Ban, J. Parsons, and W. Sippach

Nevis Laboratory, Columbia University
Irvington, NY

September, 1999

Characterization of the Coherent Noise, Electromagnetic Compatibility and Electromagnetic Interference of the ATLAS EM Calorimeter Front End Board[*]

R.L. Chase, M. Citterio, F. Lanni, D. Makowiecki, V. Radeka, S. Rescia, and H. Takai,
Brookhaven National Laboratory, Upton, NY, USA
J. Ban[†], J. Parsons and W. Sippach, Nevis Laboratory, Columbia University, Irvington, NY, USA

Abstract

The ATLAS Electromagnetic (EM) calorimeter (EMCAL) Front End Board (FEB) will be located in custom-designed enclosures solidly connected to the feedtroughs. It is a complex mixed signal board which includes the preamplifier, shaper, switched capacitor array analog memory unit (SCA), analog to digital conversion, serialization of the data and related control logic. It will be described in detail elsewhere in these proceedings. The electromagnetic interference (either pick-up from the on board digital activity, from power supply ripple or from external sources) which affects coherently large groups of channels (coherent noise) is of particular concern in calorimetry and it has been studied in detail.

1. COHERENT NOISE IN CALORIMETRY

Pick-up due to external causes can impose a serious limitation to the resolution attainable in calorimeters at certain levels of shower energy even when the level of pick-up in individual channels is small compared with the random noise. This is due to the fact that signals from a number of channels must be added to determine total shower energy. Pick-up signals tends to be correlated over a large number of nearby channels and, therefore, add linearly when sums are formed, whereas the random noise, being uncorrelated from channel to channel, adds quadratically. Thus, a pick-up signal at the level of 10% of the random noise becomes of equal importance to the noise when signals from 100 channels are added.

The coherent noise can come from a number of sources:

1. Noise on power supply lines, in particular that associated with switching power supplies.
2. Digital noise associated with the operation of logic circuits and analog-to-digital converters on the same board or nearby boards.
3. External electromagnetic interference which enters the enclosure through apertures in the shielding or which is conducted on power supply and control lines which penetrate the shielding.

1.1. Power Supply Noise

In the case of the Atlas EMCAL FEB enclosures, power supply noise has been reduced to an acceptable level by using resonant charging type switching power supplies in which the switches open only at zero current level. No increase in coherent noise has been measured with respect to linear power supplies. A separate paper in these proceedings will describe the power supplies.

By injecting radio frequency (RF) directly on the power supply lines by means of a loop antenna, it has been found that RF can couple through the power supply cables.

Shielding of the cables is being considered and its effectiveness will be studied.

1.2. Digital Noise

It is the noise being generated by:

- Control signals carrying commands into the FEB (and spurious signals from the digital activity of the control cards).
- Digital activity on the FEB itself (40MHz clock, digitizer clock, serializer clock, SCA control lines.

Digital noise can be controlled by careful shielding of the input amplifiers by means of a local Faraday cage enclosing the preamplifiers and by shielding of the input connectors.

Good grounding, including ground continuity of the connector shield to the baseplane and additional ground contacts from the FEB to the baseplane further reduce the coupling of on-board digital noise to the input of the preamplifiers.

Use of fiber optic transmission of the control signals both eliminates the coupling of unwanted signal from the control cards to the FEB and breaks ground loops created by the connection of the control electronics to the FEB.

1.3. External EMI

The effect of external electromagnetic interference depends on the enclosure design, the intensity and nature of the electromagnetic field and its frequency spectrum. In general, in the closed environment of a colliding beam detector, we will be concerned only with so-called near field radiation coming from signal and command cables

associated with other detector systems that pass close to the FEB enclosures.

2. SHIELDING PROPERTIES OF A METAL ENCLOSURE [1,2]

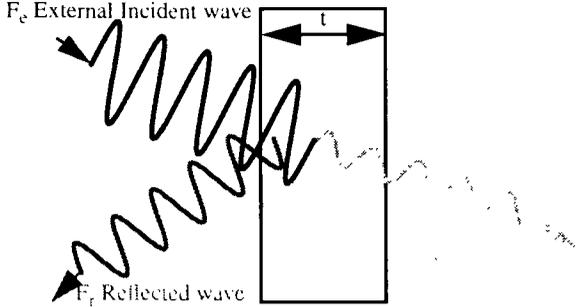The enclosure housing the FEBs is designed to shield

Fig. 1: The shielding effectiveness of a closed box is defined as the attenuation ratio of the field inside the enclosure (F_t) with respect to the external field (F_e).

the FEBs from external radiated EM fields.

Its shielding properties are defined by the "shielding effectiveness", defined as the attenuation ratio (in dB) of the field inside the enclosure with respect of the field outside as depicted in Fig1:

$$SE_{(db)} = 20 Log_{10}\left(\frac{F_t}{F_e}\right)$$

Several effects play a role, and they will be discussed in the subsequent paragraphs.

2.1. Absorption loss

It is proportional to the ratio of the thickness of the enclosure to the penetration depth of the EM wave:

$$A_{dB} = 131.4 \cdot (t \cdot \mu \cdot f)^{0.5} \qquad (\text{t in mm})$$

A = Absorption loss

t = thickness

μ = relative permeability

σ = relative conductivity (with respect to copper)

f = frequency in MHz

2.2. Reflection Loss

The reflection loss depends on the mismatch between the wave impedance Z_w = E/H and the shield impedance $Z_{shield} = \sqrt{(\omega \cdot \mu)/\sigma}$

$$R_{dB} = 20 \cdot Log_{10}\left(\frac{|Z_w|}{4 \cdot |Z_{shield}|}\right) \qquad (\text{in dB})$$

2.3. Total Shielding Effectiveness

It is the sum of the absorption and reflection loss and quantifies the quality of an enclosure. It is plotted in Fig. 2.
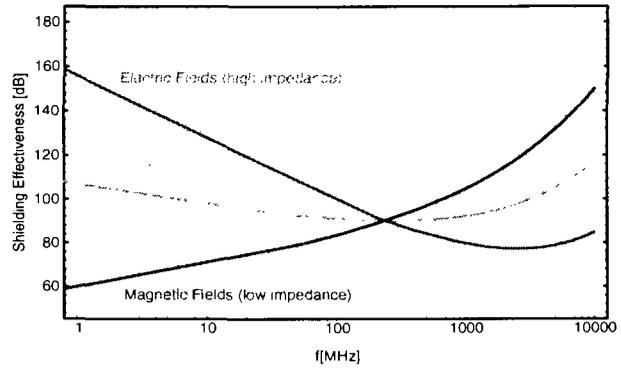

Fig. 2: Total shielding effectiveness of a closed box. It is defined as the sum of the absorption and reflection losses.

For near field magnetic fields, the most likely scenario in the densely packed environment of the calorimeter it increases with frequency. The rejection of electric fields is about 60dB higher than the one for magnetic fields at 10MHz due to the mismatch between the high wave impedance and the low shield impedance of the metallic body of the enclosure.

2.4. Effects of Apertures in an Enclosure

The shielding effectiveness of a closed box is reduced by the apertures necessary to feed control lines, power supplies etc.

The shielding (in)efficiency of n apertures is:

$$SE_{dB} = 20 \cdot Log_{10}\left(\frac{\lambda}{2 \cdot L}\right) - 20 \cdot Log_{10}(n|_{\lambda/2})$$

L = maximum linear dimension (e.g. diagonal)

λ = wavelength

n = number of slots within $\lambda\backslash 2$

The shielding effectiveness is also reduced by the seams where the front panels of the FEBs butt when inserted in the enclosure. It is improved by the presence of the cooling plates, which provide additional shielding (they can be modelled as a transmission guide below cutoff, limiting penetration of an EM wave underneath).

In conclusion, the metallic enclosure body presents a very effective reflecting mismatch to the high impedance near field environment so that electric fields are strongly attenuated before entering the enclosure.

The most troublesome potential source of interference, is likely to be near field RF magnetic fields produced by currents in nearby cables.

3. MEASUREMENT OF COHERENT NOISE

Three techniques were used in an effort to quantify the effects of external RF magnetic fields. In all cases, a magnetic field was generated by a small loop (about 15cm in diameter) driven from a 50W broadband power

amplifier excited by a variable frequency source and mounted about 25cm from the power bus side of the enclosure. The driving coaxial cable was passed through a number of ferrite toroids, acting as baluns to reduce the radiated electric field strength. A calibrated loop antenna
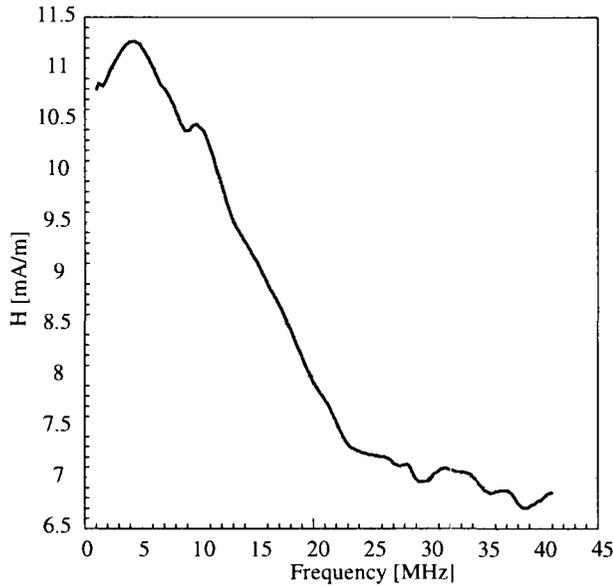

Fig. 3: Magnetic Field H measured by the monitoring antenna 25cm in front of the transmitting loop.

(COM-Power AL130) was placed 25cm in front of the transmitting loop. The signals from the 128 channels on each FEB are summed in four groups of 32 channels for trigger purposes. In one of the techniques, these sums were used, rather than the individual channel signals, to increase the level of coherent noise relative to the random noise.

3.1. Measurement of Coherent noise with a Network Analyzer

The first technique makes use of a network analyzer (HP4395). The RF output of the spectrum analyzer is connected to the power amplifier (see Fig. 4) as the source of electromagnetic interference. The calibrated antenna output is connected to the "A" input of the analyzer and the amplified sum signal is connected to the R (reference) input. The network analyzer is swept over the range of 1 to 40MHz, using a narrow filter bandwidth (100Hz). The narrow bandwidth suppresses all frequencies except the exciting frequency, and the instruments displays a plot of the RF level measured on the sum signal, normalized to the excitation field as measured by the receiving antenna.The results, normalized to the coherent noise per channel assuming an equal contribution of each channel, are shown in Fig. 5a as a solid line for the "slice" of the board (i.e. the sum top and bottom of one quarter of the FEB) nearest to the power supply bus (worst case). Fig. 5b plots the coherent noise of each slice: the noise decreases as the distance from the transmitting antenna and the
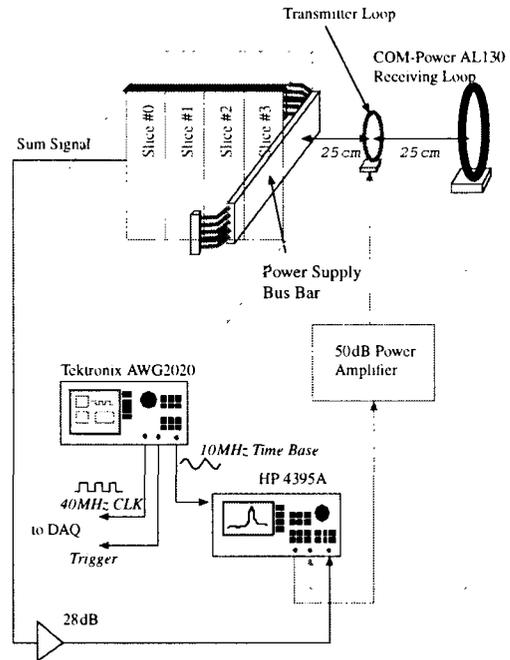

Fig. 4: Block diagram of the experimental setup to measure the coherent noise due to an external electromagnetic field by means of a network analyzer. The Tektronix AWG2020 is used to provide an external time base phase locked to the 40MHz clock to the HP4395 to phase lock the RF interference signal when necessary.

3.2. Measurement of Coherent Noise with the DAQ and Non-coherent Clock

The second technique makes use of the complete FEB digitizing and data transfer capability of the FEB data acquisition system (DAQ). The 40MHz digitizing clock is asynchronous with respect to the electromagnetic interference frequency. The RMS fluctuation of the pedestal values for all 128 channels over a large number of software generated triggers (10,000), each 32 samples deep, taken by the switched capacitor array is measured. Channels more sensitive to pick-up than the average (due, for example to less effective grounding or shielding) show higher levels of total noise. Fig. 6 shows the plot of the rms noise versus channel number for a frequency of 28.5MHz, at which the average coherent noise is maximum. It can be seen that the first half of the FEB (ch.1-64) is barely affected. The worst coherent noise is for the channels nearest to the transmitting antenna and also nearest to the slots for the power supply, the timing, trigger and control (TTC) cable and the SPAC cable.

This coherent noise is due to EMI coupling into the input of the preamplifiers: it is greatly reduced when the capacitors connected to the input of the FEB on the pedestal are removed.

The plot of Fig. 6 shows also an odd-even effect, related to the length of the pins of the right angle connector at the input of the FEB. This technique is useful

Normalized Coherent Noise per Channel

a

Network Analyzer

Coherent clock and trigger

Normalized Coherent Noise per Channel

b

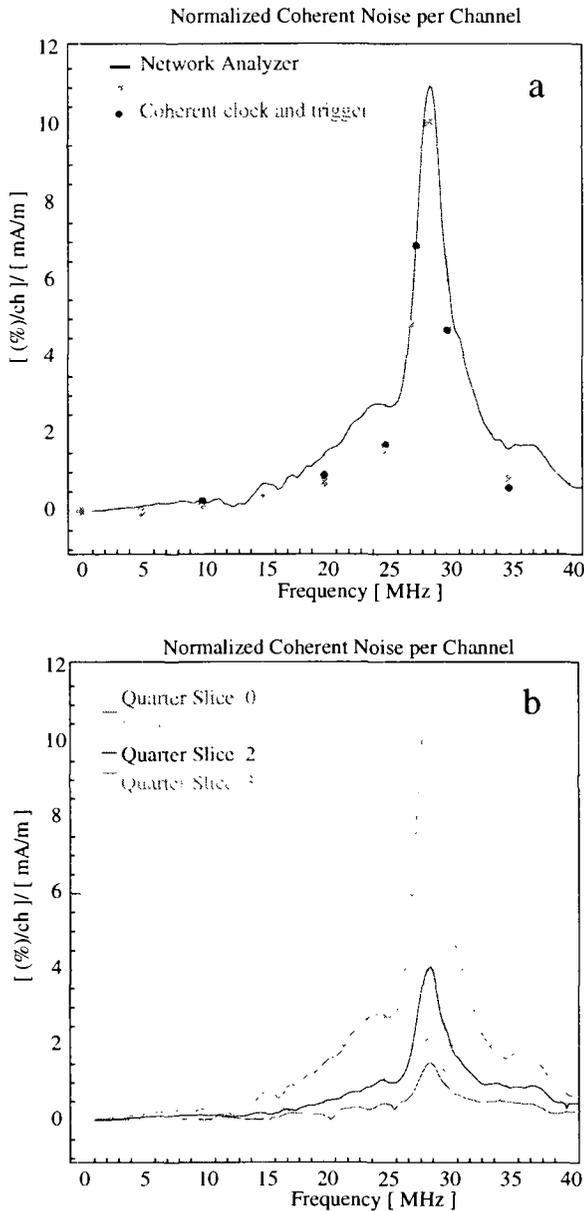Quarter Slice 0

Quarter Slice 2

Quarter Slice 3

Fig. 5: Coherent noise vs. frequency of the external RF interference normalized with respect of the measured H field

a: Noise of "slice 3" (i.e. sum of 1/4 of the FEB channels, top and bottom nearest to the power supply) measured with various techniques. Solid line: Network analyzer Squares: DAQ with non-coherent clock and trigger. Circles: DAQ and coherent clock and trigger.

b: Comparison of the coherent noise summed by "slice": the noise decreases with distance from the FEB side nearest to the transmitting antenna

for finding defects in the board design and did, in fac show that additional spring contacts between the two FEB external ground planes and the ground planes of the back-plane are very helpful, but it cannot detect a coherent

Table 1: FEB Coherent Noise

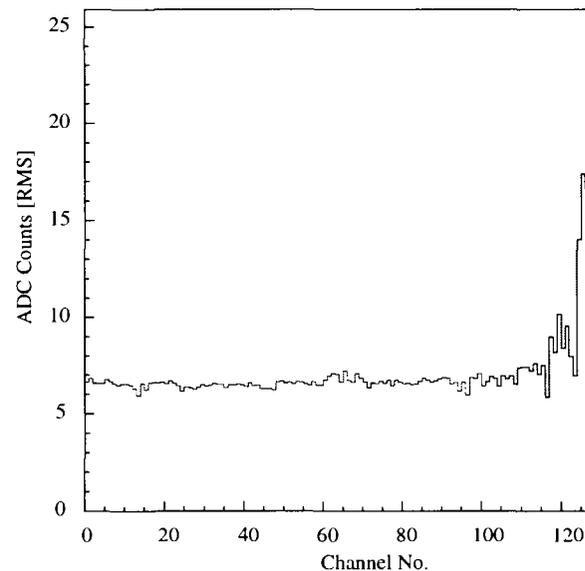| Sum type	Intrinsic FEB noise [%/ch]	External RF f=28.5 MHz H=7.2 mA/m [%/ch]
Top	3.76	37.33
Bottom	4.03	22.40
Left Half	3.69	11.21
Right Half	4.50	48.87
Top Left Quarter	4.04	10.61
Bottom Left Quarter	3.80	12.25
Top Right Quarter	5.13	34.95
Bottom Right Quarter	4.86	63.02
Slice 0, Quarter	4.54	9.06
Slice 1, Quarter	4.00	14.07
Slice 2, Quarter	4.39	24.38
Slice 3, Quarter	5.64	75.01
Total (128 ch)	3.62	29.78

Fig. 6: rms noise vs. channel number measured for an external RF at f=28.5MHz inducing a field H=7.2mA/m.

noise less than about 10% per channel of the random noise. To increase the sensitivity, digital sums over large groups of channels are formed. The rms noise in the digital sum of the data from n channels is compared with the square root of n times the average rms noise per channel. If these are equal, there is no coherent noise. The quadratic difference is a measure of the coherent noise, but it gives no indication of the source of this noise nor of its frequency spectrum.The coherent noise of the digitally generated sum of the "slice" nearest to the power supply

bus are shown as solid squares in Fig. 5a. Table 1 shows the coherent noise of various subsets of the FEB for the noise sources intrinsic to the FEB itself and for an external RF at a frequency of 28.5 MHz and a field intensity as measured at the monitoring antenna of H=7.2 mA/m. Both Table 1 and Fig. 6 show that the pick-up decreases approximately exponentially with distance from the side of the enclosure, the 1/e distance being about 8 channels. This shows that the assumption made, in the other two measurement modes, that the pick-up is uniform over 32 channels is not really valid.

3.3. Measurement of Coherent Noise with the DAQ and Coherent Clock.

The technique described in the previous paragraph is sensitive to coherent noise down to the level of 1-2 per cent of the random noise.

To increase the sensitivity, the RF interference source is phase-locked to the 40MHz sampling clock. Also the trigger is synchronized to the RF frequency. The 32 successive samples saved in the SCA plot out the waveform of the interference signal. Averaging over many events (10,000) suppresses the random noise and leaves only the coherent noise. Coherent noise measured with this method is shown as circles in Fig. 5.

4. AN EXAMPLE

The measurement of the effect of an external interference on the FEB allows an estimate of the maximum currents allowable in nearby cables.

For example assuming a sensitivity of 10%/(mA/m)/ch, the maximum field allowable to induce a 10% coherent noise per channel would be 1 mA/m. The maximum magnetic field created by two parallel wires normal to the plane of the wires is [1,3]:

$$|H| = \frac{1}{2\pi} \cdot I \cdot \frac{2d}{r^2} \qquad \text{for } d \ll r$$

where I is the current in each wire (in opposite directions, of course), d is the distance between wires and r is the distance from the wire pair. As an example, the differential current flowing in parallel wires 1mm apart necessary to create a magnetic field of 1 mA/m at a distance of 10cm is ~30 mA. However in a practical system the wires are twisted and the field will be much lower, and it will be lower still if the wire pair is shielded.

A system test has been performed to measure the possible interferences between the LAr read-out and the Transition Radiation Detector (TRT) read-out.

A board emulating the TRT driver and measuring the bit error rate at full speed was brought at the LAr test stand at BNL. Four TRT cables, each with 20 twisted pairs were looped on the side of the FEB enclosures, in the location where the TRT cables will be in the final setup.

The effect of the EMI emitted from this cable on the FEB was exceedingly small, with an increase of the average coherent noise of ~0.3%/ch at 20MHz, and only ~0.08%/ch at 40MHz.

Also the effect of the FEB and associated controls on the TRT bit error rate was so small not to generate any error over a 60 hours run at 40 Mbit/s. This corresponds to a BER<10^{-14}.

5. CONCLUSIONS

The FEB enclosure provides an effective shielding against EM fields: no effect is measured unless strong EM fields are generated with a power amplifier. The maximum effect is of the order of 10%/(mA/m)/ch at a frequency of 28.5MHz.

Its shielding effectiveness is lower for magnetic fields: the most potentially troublesome source of EMI are therefore near fields from currents in cables nearby the FEB enclosures. The openings on the enclosure and the penetrations to carry external signals to the FEB are weak spots. Possible improvements are:

• Use optoelectronics transmission whenever possible.
• Extend the Faraday cage to include the power supply bus bars, cables and switching power supplies crate.

To limit the coherent noise of the digital activity on the FEB itself careful shielding of the input connectors and ground continuity from the FEB to the baseplane are mandatory.

Low noise switching power supplies using a resonant charging technique do not add to the coherent noise in a measurable way.

6. ACKNOWLEDGEMENT

7. REFERENCES

[1]: H.W. Ott, "Noise Reduction Techniques in Electronic Systems", New York: Wiley Interscience, 1988.

[2]: A good practical reference is the product catalog of Instrument Specialties, Delaware Water Gap, PA

[3]: S. A. Shelkunoff, "Electromagnetic Fields", New York: Blaidsell, 1963.